analysis were wild-type by footprinting (perhaps because of cross-feeding in the Ty pool or because the products are required for germination) and the minimal medium–specific growth defects we detected for *hom3* and *ilv1* mutants were not detected by genomic footprinting.

18. Cultures of BY4743 ho::KanMX4 were grown at 30°C in YPD or minimal media supplemented with histidine, uracil, lysine, methionine, and adenine, in the presence of G418, and were harvested at mid-log phase. cDNA was prepared from 20 μg of polyadenylated RNA from each sample, using a dT_{21} primer and Superscript II reverse transcriptase (GibcoBRL), according to the manufacturer's recommendation. cDNA was fragmented using DNaseI (GibcoBRL), biotinylated using ddATP (NEN) and Terminal Transferase (Boehringer), and hybridized to yeast full-genome arrays (Affymetrix) as described in L. Wodicka *et al.* [*Nature Biotechnol.* **15**, 1359 (1997)]. After scanning, the average signal from each array was normalized to the average signal strength of all eight chips.
19. F. Baganz *et al.*, *Yeast* **14**, 1417 (1998).
20. Contributing groups include all authors, G. Valle, S. Kelley, J. Strathern, and D. Garfinkel.
21. EUROFAN projects B0 and B9 at www.mips.biochem.mpg.de/proj/eurofan/index.html; R. Niedenthal *et al.*, *Yeast*, in press.
22. G. Giaever *et al.*, *Nature Genet.* **21**, 278 (1999).
23. K. H. Wolfe and D. C. Shields, *Nature* **387**, 708 (1997).
24. M. Bickle, P. A. Delley, A. Schmidt, M. N. Hall, *EMBO J.* **17**, 2235 (1998); J. Corominas *et al.*, *FEBS Lett.* **310**, 182 (1992); M. A. Santos, J. J. Garcia-Ramirez, J. L. Revuelta, *J. Biol. Chem.* **270**, 437 (1995).
25. T. Y. Chow, J. J. Ash, D. Dignard, D. Y. Thomas, *J. Cell Sci.* **101**, 709 (1992); M. R. Rad *et al.*, *Yeast* **13**, 281 (1997); J. D. Brown *et al.*, *EMBO J.* **13**, 4390 (1994); A. K. Machado, B. A. Morgan, G. F. Merrill, *J. Biol. Chem.* **272**, 17045 (1997).
26. A. Yamamoto, V. Guacci, D. Koshland, *J. Cell Biol.* **133**, 85 (1996); S. D. Leidich and P. Orlean, *J. Biol. Chem.* **271**, 27829 (1996).
27. R. K. Storms *et al.*, *Genome* **40**, 151 (1997); S. J. Elledge and R. W. Davis, *Genes Dev.* **4**, 740 (1990); S. Kasahara *et al.*, *J. Bacteriol.* **176**, 1488 (1994).
28. S. P. A. Fodor *et al.*, *Science* **251**, 767 (1991); A. C. Pease *et al.*, *Proc. Natl. Acad. Sci. U.S.A.* **91**, 5022 (1994).
29. C. B. Brachmann *et al.*, *Yeast* **14**, 115 (1998).
30. We thank D. Lashkari for establishing the oligonucleotide synthesis facility, T. Nguyen, M. Sigrist, and K. Tanner for help in tetrad analysis, S. Voegeli for DNA sequence analyses, P. Koetter for distribution of deletion strains, J. Rine for helpful advice, and M.Cherry and K. Wolfe for files. E.A.W. is supported by the John Wasmuth fellowship in Genomic Analysis (HG00185-02). Supported by NIH grants HG01633, HG01627, HG00198, by an operating grant from the Medical Research Council of Canada, by grants from the European Commission (BIO4-CT97-2294), by the Swiss Federal Office for Education and Science, and by the region de Bruxelles-Capital, Belgium.

26 March 1999; accepted 7 July 1999

Early Neocortical Regionalization in the Absence of Thalamic Innervation

Emily M. Miyashita-Lin,[1]* Robert Hevner,[1]* Karen Montzka Wassarman,[2]† Salvador Martinez,[3] John L. R. Rubenstein[1]‡

There is a long-standing controversy regarding the mechanisms that generate the functional subdivisions of the cerebral neocortex. One model proposes that thalamic axonal input specifies these subdivisions; the competing model postulates that patterning mechanisms intrinsic to the dorsal telencephalon generate neocortical regions. *Gbx-2* mutant mice, whose thalamic differentiation is disrupted, were investigated. Despite the lack of cortical innervation by thalamic axons, neocortical region–specific gene expression (*Cadherin-6*, *EphA-7*, *Id-2*, and *RZR-beta*) developed normally. This provides evidence that patterning mechanisms intrinsic to the neocortex specify the basic organization of its functional subdivisions.

The mammalian neocortex is organized into regionally distinct functional subdivisions. There are two proposed mechanisms for neocortical regionalization. The protocortex hypothesis postulates that thalamic afferent fibers play an important role in neocortical regional development (*1*). On the other hand, the protomap hypothesis (*2*) postulates that regionalization of the neocortex is due to molecular differences within the neocortical ventricular zones (*3*–*7*). We investigated mice with a mutation of the *Gbx-2* gene (*8*, *9*) that disrupts thalamic histogenesis, which in turn blocks formation of thalamocortical projections.

Analysis of *Gbx-2*, *Id-4*, and *Lef-1* expression showed that *Gbx-2*–deficient mice have abnormal thalamic development. *Gbx-2* expression in the dorsal thalamus (DT) could be detected in the subventricular (SVZ) and mantle zones (MZ) (*10*). In the *Gbx-2* mutant, *Gbx-2* mRNA expression was maintained in the SVZ but was lost in the MZ (Fig. 1, E and F), suggesting that the mutant is unable to produce normal DT postmitotic cells (*Gbx-2* transcripts were detected in the mutant because the 5′ end of this gene has not been altered). This hypothesis was supported by the expression pattern of *Id-4*. The *Id-4* helix-loop-helix gene (*11*), which normally is expressed throughout the MZ of the DT, was not detectable in the DT of the *Gbx-2* mutant (Fig. 1, I and J). In addition to the apparent defect in the MZ, there was ectopic expression of *Lef-1* in the mutant. At embryonic day (E) 14.5, the *Lef-1* high mobility group box transcription factor (*12*) was expressed in the MZ of the pretectum (PT) and DT. In the *Gbx-2* mutants, *Lef-1* expression in the PT was unaffected, whereas its expression in the MZ was lost in the DT, and ectopic periventricular expression was observed (Fig. 1, M and N). Thus, by E14.5, loss of *Gbx-2* function disrupted differentiation in most, or all, of the DT.

To verify the thalamic abnormalities, we studied thalamic anatomy at postnatal day (P) 0, the day when these animals die. Histological abnormalities in the P0 *Gbx-2* mutant thalamus were even more pronounced. *Gbx-2* expression marked the lateral dorsal (LD), centromedian (CM), dorsal lateral geniculate (DLG), and reuniens (Re) nuclei (Fig. 1G). Several other nuclei also expressed *Gbx-2*, including the ventral lateral, the midline, the anteromedial, the mediodorsal, and the medial geniculate (MG) nuclei (*13*). In the mutant, there was only weak *Gbx-2* expression, which was restricted to a periventricular region (see asterisk in Fig. 1H).

Some thalamic regions of the *Gbx-2* mutants retained *Id-4* and *Lef-1* expression. *Id-4* expression marked most nuclei in the DT and the reticular nucleus (RT) of the ventral thalamus (Fig. 1K). In contrast, the *Gbx-2* mutant had greatly reduced *Id-4* expression in most areas of the DT (Fig. 1L) but retained expression in the RT, which does not express *Gbx-2* (*10*). Limited *Id-4* expression was detectable in some dorsal thalamic areas that, on the basis of their location, may correspond to the ventrobasal complex (VB) and DLG nuclei (Fig. 1L). *Lef-1* expression marked specific DT subdivisions including the DLG, VB, ventromedial (VM), and posterior (Po) nuclei (Fig. 1O). In the *Gbx-2* mutant, *Lef-1* expression was lost from most of the MZ, but unlike the wild type, its expression was found near the ventricle (arrow in Fig. 1P). Some *Lef-1*

[1]Nina Ireland Laboratory of Developmental Neurobiology, Department of Psychiatry, School of Medicine, University of California San Francisco, San Francisco, CA 94143–0984, USA. [2]Department of Anatomy and Program in Developmental Biology, School of Medicine, University of California, San Francisco, CA 94143–0452, USA. [3]Department of Morphological Sciences, Faculty of Medicine, University of Murcia, Institute of Neurosciences, University Miguel Hernandez, Alicante, Spain.

*These authors contributed equally to this work.
†Present address: Cell Biology and Metabolism Branch, National Institute of Child Health and Human Development, National Institutes of Health Building 18T, Room 101, 9000 Rockville Pike, Bethesda, MD 20892, USA.
‡To whom correspondence should be addressed. E-mail: jlrr@cgl.ucsf.edu

expression was observed in areas that we interpret as corresponding to the VB, DLG, and Po nuclei (Fig. 1P) (*13*). Thus, although most of the thalamus was defective in the *Gbx-2* mutant, there remained some areas that may correspond to thalamic nuclei that normally have reciprocal connections with the neocortex (for example, DLG, VB, Po, and MG).

To determine whether thalamocortical connections were intact in the mutant, we used 1,1′-dioctadecyl-3,3,3′,3′-tetramethylindocarbocyanine perchlorate (DiI) and immunohistochemical staining methods. Placement of a DiI crystal into the DT of E14.5 normal (*Gbx-2*$^{+/+}$ or Gbx-2$^{+/-}$) embryos labeled cell bodies and axons that project into the internal capsule (IC) (n = 5) (Fig. 2A). In E14.5 *Gbx-2*$^{-/-}$ embryos, the number of axons entering the IC was severely reduced (n = 5) (Fig. 2B). Implanted DiI in the DT at E16.5 labeled thalamocortical fibers that reach the neocortical subplate in normal animals (n = 7) (Fig. 2C), whereas thalamic fibers stopped in the IC of Gbx-2 mutants (n = 5) (Fig. 2D). Placement of DiI in the DT of normal mice at E18.5 (Fig. 2E) or P0 (*14*) labeled thalamocortical fibers anterogradely and corticothalamic fibers and their cell bodies retrogradely (n = 4). In most mutant cases (n = 5), no labeled axons were observed in the cortex (Fig. 2F). In only one mutant (E18.5) did a few thalamocortical fibers innervate the subplate; this sparse innervation was detected in both hemispheres (*14*).

Finally, placement of DiI in the normal neocortex at E18.5 (*14*) or P0 (Fig. 2G) labeled thalamocortical fibers and their cell bodies retrogradely (inset in Fig. 2G) and cerebral peduncle fibers (Fig. 2G) and corticothalamic fibers (*14*) anterogradely (n = 4). In contrast, no retrograde labeling of thalamic neurons was observed after DiI injections into the *Gbx-2* mutant neocortex in six of seven cases (*14*). In the single exceptional case, both corticothalamic and thalamocortical projections were present in both hemispheres, showing that this animal did not have a fully penetrant defect in its thalamus.

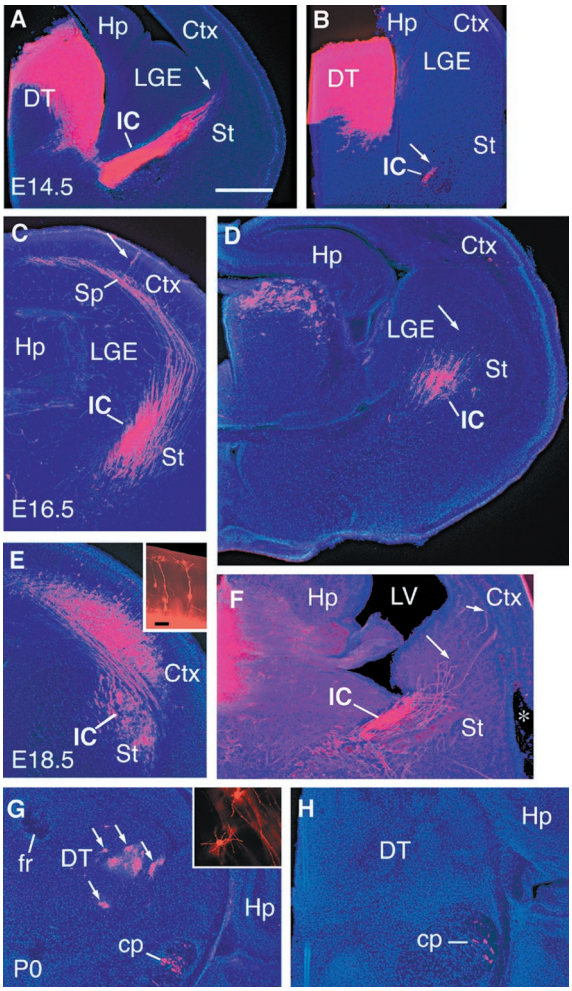

Fig. 2. Loss of neocortical innervation by the thalamus in *Gbx-2* mutants. DiI fluorescence is in pink; the tissue is counterstained in blue with DAPI (4,6 diamidino-2-phenylindole). All panels are oriented with medial to the left. (Left) Gbx-2$^{+/+}$ or Gbx-2$^{+/-}$. (Right) Gbx-2$^{-/-}$. (**A** and **B**) DiI injections in the DT at E14.5 label thalamocortical fibers that reach the striatopallial angle in normal mice [arrow in (A)]; in *Gbx-2* mutants, these fibers extend only into the midportion of the IC [arrow in (B)]. (**C** and **D**) DT injections of DiI at E16.5 retrogradely label some neocortical cells [arrow in (C)]. In *Gbx-2* mutants, thalamocortical fibers extend no farther than the lateral IC [arrow in (D)]. DiI labeling in the cortex (Ctx) is nonspecific. (**E** and **F**) DT injections of DiI at E18.5; in controls (E), thalamic fibers that innervated the cortex are labeled, and neocortical pyramidal neurons are retrogradely labeled [inset in (E)]. In *Gbx-2* mutants (F), most thalamic fibers remain within the IC [long arrow in (F)], although a few approach the cortex [short arrow in (F)]. The asterisk in (F) indicates an aberrant extension of the lateral ventricle (LV) observed in some *Gbx-2*$^{-/-}$ forebrains. (**G** and **H**) Labeling of neurons in the DT from DiI injections into the cortex at P0. Retrogradely labeled cells are visible in the normal DT [arrows and inset in (G)] but not in the mutant DT. In the mutant, corticothalamic fibers did not reach that thalamus (*14*), whereas the cerebral peduncle (cp) was present (G and H). fr, fasciculus retroflexus; Hp, hippocampus; LGE, lateral ganglionic eminence; St, striatum. Scale bars: (A), 500 mm (all panels shown at the same scale); inset in (E), 50 mm (both insets shown at the same scale) (*26*).

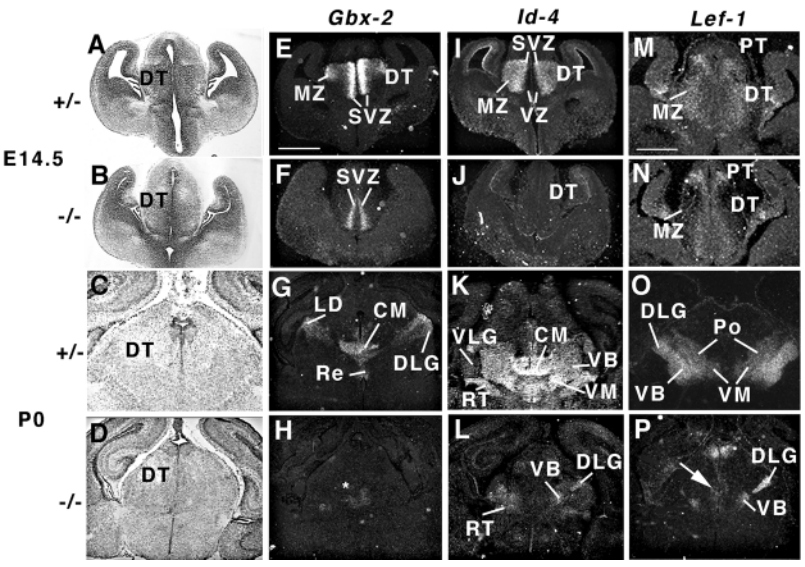

Fig. 1. Gene expression patterns in the thalamus of E14.5 and P0 *Gbx-2* mutant and control brains. The age and genotype of the sections are indicated on the left; the gene markers are indicated at the top of the figure. (**A** to **D**) Nissl stain reference sections. (**E** to **H**) Expression of *Gbx-2*. (**I** to **L**) *Id-4* expression. (**M** to **P**) *Lef-1* expression; the arrow in (P) highlights the ectopic periventricular expression. CM, centromedian; VLG, ventral lateral geniculate; VZ, ventricular zone. (*25*). Scale bars: (E), 0.75 mm [same for (F) to (L), (O), and (P)]; (M), 0.53 mm [same for (N)].

To confirm the DiI results, we hemisected some of the P0 brains; one hemisphere was used for DiI tracing, and the other was used to study the expression of thalamocortical axonal markers [that is, serotonin (5HT), P450c17, and calretinin]. In each case, the immunohistochemical and DiI results were concordant. 5HT immunohistochemistry (*15*) revealed that only the control animal had staining of the SP/CP (subplate/cortical plate) (Fig. 3, A and B). Immunohistochemical analysis of P450c17, an enzyme that converts pregnenolone to DHEA (dehydroepiandrosterone), showed thalamocortical fibers in the intermediate zone (IZ) and SP in normal mice (*16*) but not in *Gbx-2* mutants (Fig. 3, C and D). Whereas the thalamocortical pathway was disrupted, other P450c17-labeled cortical axons, such as the angular bundle (AB), appeared unaffected (Fig. 3D) (*13*).

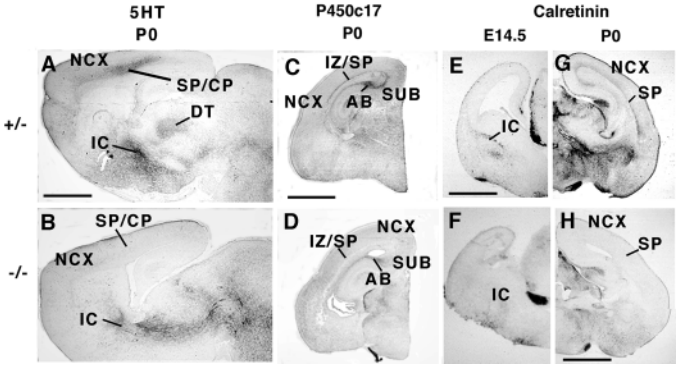

Fig. 3. Immunohistochemical analysis of thalamocortical projections in *Gbx-2* mutants: expression of 5HT and P450c17 at P0 and calretinin at P0 and E14.5. The genotypes are indicated on the left-hand side; the markers and age of the brains are listed at the top. (**A** and **B**) 5HT expression in saggital sections of P0 brains. 5HT expression was lost in the SP/CP of the mutant. (**C** and **D**) P450c17 expression at P0 in coronal sections; expression was lost in the fibers in the IZ/SP of the mutant, whereas expression in the AB in the subiculum (SUB) was preserved (D). (**E** and **F**) Calretinin expression at E14.5 in coronal sections revealed that labeled fibers in the IC were absent in the mutant. (**G** and **H**) Calretinin expression at P0 in coronal sections revealed that labeled fibers in the SP were absent in the mutant. NCX, neocortex (*27*). Scale bars: (A), 1.3 mm; (C), 1.0 mm [same for (D)]; (E), 0.83 mm [same for (F)]; and (H), 1.2 mm [same for (G)].

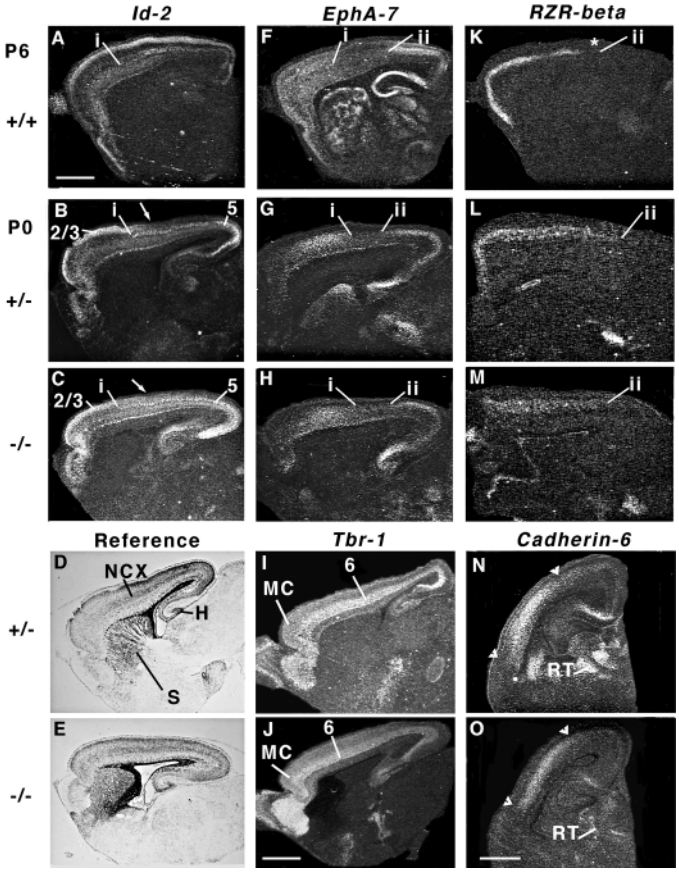

Fig. 4. In situ hybridization shows that intraneocortical gene expression boundaries and neocortical lamination are not affected by the lack of thalamic input in *Gbx-2* mutants. Genotypes are indicated on the left and gene markers on top. Nissl-stained sections are shown (**D** and **E**). Expression of *Id-2*, *EphA-7*, and *RZR-beta* at P6 (**A**, **F**, and **K**) and P0 (**B**, **G**, and **L**) respects two intraneocortical boundaries: i and ii. These boundaries appear normal in P0 *Gbx-2* mutants (**C**, **H**, and **M**). *Cadherin-6* expression (P0) in parietal neocortical areas 1 and 2 (arrowheads) in the mutant matches normal expression (**N** and **O**). *Tbr-1* expression (P0) shows its normal strong expression in the motor cortex (MC) and layer 6 in the mutant (*28*) (**I** and **J**). The asterisk in (K) indicates an area where low *RZR-beta* expression is detectable. Scale bars: (O), 0.88 mm [same for (N)]; (J), 0.7 mm [same for (B) to (E), (G) to (I), (K), and (L)]; and (A), 1.2 mm [same for (F) and (K)].

We studied neocortical regionalization and laminar organization using the expression of *Id-2*, *EphA-7*, *RZR-beta*, *Cadherin-6*, and *Tbr-1* at P0 and found no obvious differences in the cortical expression of these genes between control (Fig. 4, B, G, I, L, and N) and *Gbx-2* mutants (Fig. 4, C, H, J, M, and O). Expression of *Id-2* (Fig. 4, A to C), which encodes a helix-loop-helix protein, demarcates functionally important regional boundaries and layers in the cortex (*5*). For instance, layer 5 expression has a rostral boundary at the sensory-motor limit at P0 and P6 (*18*) (see boundary "i" in Fig. 4A). Expression of *EphA-7* (Fig. 4, F to H), a receptor protein tyrosine kinase that is involved in axon guidance (*19*), has two neocortical expression boundaries at P6 and P0: Boundary i approximates the sensory-motor limit (*18*); boundary "ii" is within the sensory neocortex (Fig. 4, F to H). Boundary ii has not been mapped with respect to neocortical subdivisions. Expression of *RZR-beta*, which encodes an orphan nuclear receptor (*20*), has a limit that also approximates boundary ii (Fig. 4, K to M). Expression of *Cadherin-6* (Fig. 4, N and O), which encodes a cell-surface ad-

hesion protein, demarcates parietal areas 1 and 2 and temporal area 1 (*21*). Finally, laminar development was further assessed by studying *Tbr-1*, a T-box gene, which is expressed in layer 6 (*5*) (Fig. 4, I and J).

In summary, *Gbx-2* mutant mice have a block in DT differentiation that affects most thalamic regions and that disrupts growth of thalamocortical axons. Despite the absence of thalamic afferents, neocortical regionalization and histogenesis were indistinguishable from control mice at P0. This provides strong evidence that regional specification within the neocortex is controlled at least in part by patterning mechanisms that are intrinsic to the telencephalon. The molecular regulation of patterning in the telencephalon is poorly understood. Candidate cortical patterning centers include the dorsal midline, which expresses bone morphogenetic proteins and *Wnts*, and the rostral midline, which expresses fibroblast growth factor–8 (*22*). These tissues may control the expression of transcription factors that are implicated in regulating cortical regionalization (for example, *Emx-1*, *Emx-2*, *Otx-1*, *Bf-1*, *Gli-3*, *Tlx*, and *Tbr-1*) (*18*, *23*). Although some early steps in neocortical molecular regionalization (even within the sensory neocortex) and lamination may be largely independent of thalamic influence, it is likely that thalamic input regulates later steps in neocortical development, such as neuronal maturation, and the formation of neocortical modules (for example, barrels) and association cortices. This latter hypothesis is based on the evidence that afferent fibers can regulate the architecture and gene expression of thalamic and cortical tissues (*24*). Unfortunately, because *Gbx-2* mutants die on P0, we need to devise methods to study the mutant neocortex in more mature animals to investigate the role of thalamic afferents on postnatal neocortical development.

References and Notes

1. D. D. M. O'Leary, *Trends Neurosci.* **12**, 400 (1989).
2. P. Rakic, *Science* **241**, 170 (1988).
3. R. T. Ferri and P. Levitt, *Cereb. Cortex* **3**, 187 (1993).
4. M. Cohen-Tannoudji, C. Babinet, M. Wassef, *Nature* **368**, 460 (1994).
5. A. Bulfone *et al.*, *Neuron* **15**, 63 (1995).
6. F. Nothias, G. Fishell, A. Ruiz i Altaba, *Curr. Biol.* **8**, 459 (1998).
7. Y. Arimatsu *et al.*, *Proc. Natl. Acad. Sci. U.S.A.* **89**, 8879 (1992).
8. The Gbx-2 mutant allele lacks the homeobox; see (*9*).
9. K. M. Wassarman *et al.*, *Development* **124**, 2923 (1997).
10. A. Bulfone *et al.*, *J. Neurosci.* **13**, 3155 (1993).
11. V. Riechmann, I. Van Cruchten, F. Sablitzky, *Nucleic Acids Res.* **22**, 749 (1994).
12. A. Travis, A. Amsterdam, C. Belanger, R. Grosschedl, *Genes Dev.* **5**, 880 (1991).
13. E. M. Miyashita-Lin, R. F. Hevner, J. L. R. Rubenstein, unpublished results.
14. R. F. Hevner, E. M. Miyashita-Lin, J. L. R. Rubenstein, in preparation.
15. C. Lebrand *et al.*, *Neuron* **17**, 823 (1996).
16. N. A. Compagnone, A. Bulfone, J. L. R. Rubenstein, S. H. Mellon, *Endocrinology* **136**, 5212 (1995).
17. M. Fonseca, J. A. Del Rio, A. Martinez, S. Gomez, E. Soriano, *J. Comp. Neurol.* **361**, 177 (1995); C. Frassoni, P. Arcelli, M. Selvaggio, R. Spreafico, *Neuroscience* **83**, 1203 (1998).
18. J. L. R. Rubenstein *et al.*, *Cereb. Cortex*, in press.
19. T. Mori, A. Wanaka, A. Taguchi, M. Kazumasa, M. Tohyama, *Mol. Brain Res.* **34**, 154 (1995).
20. N. Schaeren-Wiemers, E. Andre, J. P. Kapfhammer, M. Becker-Andre, *Eur. J. Neurosci.* **9**, 2687 (1997).
21. S. C. Suzuki, T. Inoue, Y. Kimura, T. Tanaka, M. Takeichi, *Mol. Cell. Neurosci.* **9**, 433 (1997).
22. Y. Furuta, D. W. Piston, B. L. Hogan, *Development* **124**, 2203 (1997); J. A. Golden *et al.*, *Proc. Natl. Acad. Sci. U.S.A.* **96**, 2439 (1999); E. A. Grove, S. Tole, J. Limon, L. Yip, C. W. Ragsdale, *Development* **125**, 2315 (1998); J. L. R. Rubenstein and P. A. Beachy, *Curr. Opin. Neurobiol.* **8**, 18 (1998).
23. T. Frantz, *Acta Anat.* **150**, 38 (1994); M. Qiu *et al.*, *Dev. Biol.* **178**, 174 (1996); S. Xuan *et al.*, *Neuron* **14**, 1141 (1995); M. Pellegrini, A. Mansouri, A. Simeone, E. Boncinelli, P. Gruss, *Development* **122**, 3893 (1996); A. Stoykova, C. Walther, R. Fritsch, P. Gruss, *ibid.*, p. 3453; D. Acampora, V. Avantaggiato, F. Tuorto, A. Simeone, *ibid.* **124**, 3639 (1997); A. P. Monaghan *et al.*, *Nature* **390**, 515 (1997); M. Yoshida *et al.*, *Development* **124**, 101 (1997).
24. L. C. Katz and C. J. Shatz, *Science* **274**, 1133 (1996); Y. Gitton, M. Cohen-Tannoudji, M. Wassef, *Cereb. Cortex*, in press.
25. Gbx-2–deficient mice embryos were obtained from timed matings where plugs found the next morning were designated E0.5. (Animals were killed according to University of California, San Francisco animal care guidelines.) Cryostat sections (10 μm) from 4% paraformaldehyde-fixed brains were processed for in situ hybridization (*10*) with ^{35}S-labeled riboprobes encoding Gbx-2, Id-4, and Lef-1.
26. A. Bulfone *et al.*, *Neuron* **21**, 1273 (1998).
27. Immunohistochemistry on 10-μm cryostat sections was performed as described in (*16*) with rabbit antibodies to 5HT (1:5000), Incstar P450c17 (1:1000) (*16*), or calretinin (1:2000) (Chemicon) revealed with biotinylated goat antibody to rabbit 1:200 (Vector), followed by peroxidase staining with the VIP kit (Vector).
28. Each probe was tested on two to three different mutants and four different wild-type animals; typically, eight to nine different section planes were studied from each brain with each probe.

29. We thank G. Martin for the *Gbx-2* mutant mice, S. Mellon for antiserum to P450c17, M. Takeichi for cadherin-6, R. Grosschedl for Lef-1, M. Israel for Id-4, S. McConnell for RZR-beta, and A. Wakana for EphA-7 plasmids. This work was supported by the research grants to J.L.R.R. from: Nina Ireland, March of Dimes, the National Alliance for Research on Schizophrenia and Depression, the John Merck Fund, the Human Frontiers Science Program, the National Institute of Neurological Disorders and Stroke (NINDS) (grant NS34661-01A1) and the National Institute of Mental Health (grants RO1 MH49428-01, RO1 MH51561-01A1, and K02 MH01046-01), to R.F.H. from NINDS (grant K08NS01973), and to E.M.M. from NINDS (grant 1 F32 NS10536-01).

11 February 1999; accepted 25 June 1999